

***Drosophila melanogaster* linker histone dH1 is required for transposon silencing and to preserve genome integrity**

Olivera Vujatovic¹, Katrin Zaragoza¹, Alejandro Vaquero¹, Oscar Reina², Jordi Bernués¹ and Fernando Azorín^{1,*}

¹Institute of Molecular Biology of Barcelona, CSIC and Institute for Research in Biomedicine, IRB Barcelona and ²Bioinformatics and Biostatistics Unit, Institute for Research in Biomedicine, IRB Barcelona, Baldiri Reixac, 10-12, 08028 Barcelona, Spain

Received November 30, 2011; Revised February 1, 2012; Accepted February 22, 2012

ABSTRACT

Histone H1 is an intrinsic component of chromatin, whose important contribution to chromatin structure is well-established *in vitro*. Little is known, however, about its functional roles *in vivo*. Here, we have addressed this question in *Drosophila*, a model system offering many advantages since it contains a single dH1 variant. For this purpose, RNAi was used to efficiently deplete dH1 in flies. Expression-profiling shows that dH1 depletion affects expression of a relatively small number of genes in a regional manner. Furthermore, depletion up-regulates inactive genes, preferentially those located in heterochromatin, while active euchromatic genes are down-regulated, suggesting that the contribution of dH1 to transcription regulation is mainly structural, organizing chromatin for proper gene-expression regulation. Up-regulated genes are remarkably enriched in transposons. In particular, R1/R2 retrotransposons, which specifically integrate in the rDNA locus, are strongly up-regulated. Actually, depletion increases expression of transposon-inserted rDNA copies, resulting in synthesis of aberrant rRNAs and enlarged nucleolus. Concomitantly, dH1-depleted cells accumulate extra-chromosomal rDNA, show increased γ H2Av content, stop proliferation and activate apoptosis, indicating that depletion causes genome instability and affects proliferation. Finally, the contributions to maintenance of genome integrity

and cell proliferation appear conserved in human hH1s, as their expression rescues proliferation of dH1-depleted cells.

INTRODUCTION

Linker histone H1 is a main component of eukaryotic chromatin. *In vitro* studies showed that histone H1 binds to nucleosome core particles near the exit/entry sites of linker DNA, determines nucleosome core particle spacing and facilitates folding of nucleosomes into a higher-order structure, the ~30 nm chromatin fibre (1–8). It has also been shown that histone H1 strongly inhibits *in vitro* nucleosome mobility and transcription (9–11).

In vivo analysis of histone H1 functions remains, however, elusive. In unicellular eukaryotes, histone H1 appears to be dispensable for cell division and growth. In *Saccharomyces cerevisiae*, disruption of the 'H1-like' *Hho1* gene does not significantly affect chromatin structure, showing no major growth effects (12–14). Similarly, histone H1 has also been found dispensable for cell growth and viability in other unicellular organisms containing more canonical histone H1s, such as *Aspergillus nidulans* and *Tetrahymena* (15,16). On the other hand, studying histone H1 functions in metazoans is especially difficult, as most species contain multiple variants (17), which play redundant as well as specific functions. For instance, mice contain at least eight non-allelic variants that are encoded by single-copy genes and show differential expression patterns during development and differentiation. Null mutants for one or two of the six somatic mice H1 variants develop normally (18,19), indicating

*To whom correspondence should be addressed. Tel.: +34 93 4034958; Fax: +34 93 4034979; Email: fambmc@ibmb.csic.es

Present address:

Alejandro Vaquero, Chromatin Biology Laboratory, Cancer Epigenetics and Biology Program (PEBC), Bellvitge Biomedical Research Institute (IDIBELL), 08908 L'Hospitalet de Llobregat, Barcelona, Spain.

that expression of individual variants is compensated to maintain normal histone H1-stoichiometry and function. Similarly, in chicken DT40 cells, knocking out five of the six histone H1 variants shows no major phenotypic effects (20,21). However, compensatory effects are insufficient to account for the loss of three variants in mice, as triple mutant embryos have highly reduced histone H1 content and show multiple abnormalities, dying at E11.5 (22). Finally, knock-down experiments in human breast cancer T47D cells revealed variant-specific effects (23).

Drosophila melanogaster constitutes an attractive experimental model to analyse histone H1 functions *in vivo* because it contains a single variant, dH1 (24,25). However, classical genetic approaches cannot be used to obtain mutant conditions, as dH1 is encoded by the multicopy *His1* gene family that is composed by multiple copies located within the tandemly repeated units of the histone cluster. For this purpose, we used an RNAi strategy to induce strong dH1 depletion in flies either ubiquitously or at specific tissues and stages during development. Others used earlier a similar approach to successfully deplete dH1 *in vivo*, showing that it is an essential protein, which plays a major role in heterochromatin assembly and the structural organization of polytene chromosomes (26,27).

Here, we report on the contribution of dH1 to gene expression and genome stability. Our results show that dH1 depletion up-regulates expression of inactive genes, preferentially those located in heterochromatin, while it down-regulates expression of active euchromatic genes. Our results also show that transposable elements (TEs) are strongly up-regulated in the absence of dH1, indicating that dH1 is required for their silencing. In particular, dH1 depletion up-regulates expression of R1 and R2 retrotransposons, which are specifically integrated in the rDNA locus (28–30), resulting in an increased rDNA transcription and enlarged nucleolar structure. In addition, cells lacking dH1 accumulate extra-chromosomal rDNA circles (ecc^{rDNA}), show increased γ H2Av content, stop proliferation and activate apoptosis. Altogether, these results indicate that dH1 depletion causes genome instability and affects cell proliferation. Finally, we also show that three different human H1 variants partially rescue proliferation of cells lacking dH1, suggesting that the contributions of histone H1 to maintenance of genome integrity and normal cell proliferation are conserved functions in human H1s.

MATERIALS AND METHODS

Antibodies

Rabbit α dH1 antibody was kindly provided by Dr Kadonaga. α fibrillarlin (Abcam, ab4566), α actin (Sigma, A 2066), α tubulin (Millipore, LV1770313), α γ H2Av (Rockland, 600-401-914), α H3S10P (Millipore, LV1508850), α HA (Roche, 3F10) and α caspase-3 (Cell Signaling, Asp175) antibodies are commercially available.

Fly stocks and genetic procedures

his1^{RNAi} was constructed by crossing lines 31617R-2 and 31617R-3 from NIG-FLY, which carry UAS_{GAL4}-

hsRNA^{*His1*} constructs inserted in the 2 and X chromosome, respectively. In some experiments, *his1^{RNAi}* flies containing a single UAS_{GAL4}-hsRNA^{*His1*} construct inserted in the X-chromosome (31617R-3) were used. To obtain lines expressing human hH1.0, hH1.2 and hH1.4 variants, the corresponding Ct-HA tagged constructs, kindly provided by Dr Jordan (23), were cloned into pUASattb and transgenic flies were obtained by site-directed integration into chromosome 3 using 3R-86Fb embryos (31). *GFP^{RNAi}* line was provided by Dr Espinàs. *ptc*-GAL4, *nub*-GAL4, *Act5C*-GAL4 and UAS_{GAL4}-Dcr2 lines are described in Bloomington Stock Center. *su(var)3-9⁰⁶* flies are described in (32).

To induce dH1 depletion, appropriate crosses were kept at 25°C for 48–72 h and, then, transferred to 29°C, except for expression-profiling experiments, where crosses were kept at 29°C all the time. To visualize wings, adult flies were stored overnight in 75% ethanol, 25% glycerol solution, mounted to slides and visualized with a Nikon E600 microscope and Olympus DP72 camera.

When the ability of human hH1.0, hH1.2 and hH1.4 variants to rescue dH1 depletion was determined, appropriate crosses were kept at 25°C until hatching of adult flies. Wings were mounted and wing length calculated with the SZX16 stereomicroscope and XC50 camera (Olympus) using the cellD software (Olympus). Wing length was measured drawing a line from the ventral wing-edge to the dorsal edge of the L3 vein. When no veins were discernible, a line was drawn from the dorsal to the ventral wing border.

Expression profiling analysis

For expression profiling, *Drosophila* Genome 2.0 GeneChip (Affymetrix) were hybridized with cDNA prepared from total RNA obtained from wing imaginal discs of female blue staged third-instar larvae (33). Three replicates were processed for each of the following genotypes: (i) mutant *his1^{RNAi}*; *Act5C*-GAL4; (ii) control *his1^{RNAi}* and *Act5C*-GAL4, to account for unspecific effects due to the UAS_{GAL4}-hsRNA^{*His1*} and *Act5C*-GAL4 insertions and (iii) control *GFP^{RNAi}*; *Act5C*-GAL4, to account for unspecific effects due to hyperactivation of RNAi. GeneChips were scanned in a GeneChip Scanner 3000 (Affymetrix). We used Bioconductor (34) to perform RMA background correction, quantile normalization and RMA summarization using the *rma* function from the oligo-package to obtain probe-set expression estimates (35).

For differential expression analyses, a semi-parametric empirical Bayes procedure based on moderated *t*-tests (36) was performed, setting the Bayesian FDR at 5% (37). Four pair-wise comparisons were performed: M versus H1, M versus Actin, M versus GFP and M versus C, where M was the mutant sample, H1 was the *his1^{RNAi}* control, Actin was the *Act5C*-GAL4 control, GFP was the *GFP^{RNAi}*, *Act5C*-GAL4 control and C accounts for the average probe-set expression estimates of H1, Actin and GFP samples. Additionally, we established fold change thresholds of $|FC|_{MvsC} > 2.5$ and $|FC|_{MvsH1, MvsActin, MvsGFP} > 1.5$. Finally, only probe sets showing also fold changes with the same sign in each pair-wise comparison were considered as

differentially expressed. To assess evolution on the proportion of up- and down-regulated probe sets as a function of the change in expression, we also applied fold change thresholds of $|FC|_{MvsC} > 2$ and $|FC|_{MvsH1, MvsActin, MvsGFP} > 1.4$; $|FC|_{MvsC} > 1.75$ and $|FC|_{MvsH1, MvsActin, MvsGFP} > 1.35$; $|FC|_{MvsC} > 1.5$ and $|FC|_{MvsH1, MvsActin, MvsGFP} > 1.3$.

In order to explore patterns of deregulation around differentially expressed genes, results were first summarized to gene level by computing \log_2 fold change means and chromosomal locations for each gene were obtained using the biomaRt package (38) with *D. melanogaster* gene information from the Ensembl gene mart (March 2010 archive). Fold changes were retrieved for each up- or down-regulated gene and also for each gene in an arbitrarily defined window of the 40 upstream and 40 downstream closest genes. GSEA was also used to determine enrichment in up- and down-regulated genes within 0.5, 1 and 5 kb of up-regulated genes (GSEA *P*-value ≤ 0.001 , FDR *q*-value ≤ 0.005 ; see below). Genomic dH1 distribution was determined in S2 and BG3 cells using ChIP-chip data from modEncode (www.modencode.org). Positional information was annotated using the Bioconductor package ChIPpeakAnno (39) using the March 2010 archive of the Ensembl genes mart. This same source was used to map FlyBase gene IDs as returned by ChIPpeakAnno to Affymetrix Drosophila Genome 2.0 GeneChip probe sets.

Gene set enrichment analysis (GSEA)

The pre-ranked list GSEA tool was used to perform the Gene Set Enrichment Analysis (40,41). In this type of analysis, all probe sets in the array are ranked according to their change in expression, from the most up-regulated to the most down-regulated. Then, an enrichment-score is calculated to measure the enrichment of a given gene set as a function of the change in expression. This enrichment score is a cumulative sum over ranked genes: as we walk down the ranked list, sum gets increased when a gene is in the gene set, and decreased otherwise. Magnitude of increment depends on correlation of gene with phenotype. The enrichment score is set as the maximum deviation from zero of the cumulative sum. In our case, all probe sets in the array were ranked according to their global-fold change (pair-wise comparison of mutant samples against average expression of all control groups). Transposon ($n=78$) and heterochromatic ($n=183$) probe set lists, determined using the NetAffx Affymetrix annotation webpage for the GeneChip Drosophila Genome 2.0 Array (<http://www.affymetrix.com/analysis/netaffx/index.affx>) were used as gene sets for assessing transposon and heterochromatic enrichment. Also, three other lists ($n=167$, $n=214$ and $n=506$) containing probe sets within 0.5, 1 and 5 kb, respectively from up-regulated probe sets ($|FC| > 2.5$) were tested with GSEA to further assess regional up-regulation. Pre-ranked GSEA algorithm was run using 1000 permutations and the weighted statistic option.

Immunostaining experiments

Immunostaining of wing imaginal discs and salivary glands was performed as described earlier (42). Briefly,

larvae were dissected in cold PBS and fixed for 20 min at room temperature in PBS, 4% *para*-formaldehyde. After washing and blocking with PBS, 0.3% Triton, 2% BSA, samples were incubated at 4°C over-night with the indicated antibodies. For visualization, slides were mounted in Mowiol (Calbiochem–Novabiochem) containing 0.2 ng/ml DAPI (Sigma) and visualized on a confocal microscope Leica SPE.

Hirt *ecc*^{DNA} isolation and detection

Hirt extracts were prepared from approximately 100 imaginal discs and salivary glands from third instar larvae. Dissected organs were frozen and collected in liquid nitrogen. Samples were resuspended in 250 μ l Hirt buffer (0.6% SDS, 10 mM EDTA, pH 8) and incubated for 10 min at room temperature. Afterwards, NaCl was added to a final 1 M concentration and incubated over-night at 4°C. Following centrifugation at 14000g for 40 min at 4°C, supernatants containing *ecc*^{DNA} were kept and DNA was extracted three times with phenol-chloroform and precipitated with ethanol. *ecc*^{DNA} content was determined by qPCR using appropriate primers (Supplementary Table S3).

RESULTS

dH1 depletion has a dual effect on gene expression

To analyse the contribution of dH1 to the regulation of gene expression, we performed RNAi knock-down experiments in flies. For this purpose, we used transgenic *his1*^{RNAi} flies carrying two UAS_{GAL4}-*hsRNA*^{*His1*} constructs of the coding region of *His1* that, upon crossing to flies expressing GAL4, generate siRNAs to silence *His1* expression. In some cases, a UAS_{GAL4}-*Dcr2* construct expressing the RNAi component *Dcr2* was used to increase siRNAs production and, therefore, depletion (see ‘Materials and Methods’ section for a description of the strains used). dH1 depletion was either induced ubiquitously, by crossing *his1*^{RNAi} flies to flies carrying an *Actin5C*-GAL4 driver, or specifically at the anterior/posterior (A/P)-border and the pouch region of wing imaginal discs, by crossing to flies carrying *ptc*-GAL4 and *nub*-GAL4 drivers, respectively. Immunostaining experiments using specific α dH1 antibodies showed strong dH1 depletion (Supplementary Figure S1A). As shown by western blot analyses, depletion induced by *Actin5C*-GAL4 and *nub*-GAL4 reduces dH1 content by ~90 and 60%, respectively (Supplementary Figure S1B). Over-expression of *Dcr2* increases depletion by *nub*-GAL4 to ~75% (Supplementary Figure S1B). As reported earlier by others (26), dH1 depletion strongly compromises fly viability, as ubiquitous dH1-depletion induced by *Actin5C*-GAL4 results in strong lethality at late larval stage (81%) and no adult flies are recovered. As it was also reported earlier (26), dH1 depletion severely perturbs the structure of polytene chromosomes, which lack the characteristic banding pattern, are thinner and lose adhesion at some regions, and show altered chromocentre organization, frequently containing multiple HP1 foci (Supplementary Figure S2).

Next, to determine the effects of dH1 depletion on gene expression, we performed expression-profiling experiments in wing imaginal discs from third-instar larvae, where ubiquitous dH1 depletion was induced by *Act5C-GAL4* that, as mentioned above, reduces dH1 content by ~90%. This strong depletion affects expression of a relatively small number of genes, as ~850 genes are differentially expressed (DE-genes) by more than 1.5-fold ($|FC| > 1.5$) and only 250 genes show $|FC| > 2.5$ (Figure 1A and Supplementary Table S1). In addition, the number of DE-genes up-regulated in *his1^{RNAi}* knockdown flies is similar to that of down-regulated ones (Figure 1A and Supplementary Table S1). From all DE-genes changing expression by $|FC| > 1.5$, ~55% are up-regulated and 45% are down-regulated. However, up-regulated genes change expression more strongly than down-regulated ones, as they account for ~92% of DE-genes that change expression by $|FC| > 2.5$ (Figure 1A). These effects are likely direct since dH1 is broadly distributed throughout the genome (43,44). As a matter of fact, ~97% of DE-genes detected in *his1^{RNAi}* knockdown flies ($|FC| > 1.5$) are enriched in dH1 in SL2 and/or BG3 cells that, on the other hand, show highly overlapping dH1 genomic distributions (Figure 1B). A main difference between up- and down-regulated DE-genes is their levels of expression in control wild-type flies, as down-regulated DE-genes are more expressed than

up-regulated ones (Figure 1C). In fact, up-regulated DE-genes are enriched in silenced heterochromatic genes (Figure 2). In addition, dH1 depletion affects gene expression in a regional manner, as genes flanking strongly up-regulated genes ($FC > 2.5$) are also up-regulated (Figure 1D). This effect, which extends for ~40 genes (20 up- and 20 down-stream), is not observed with regular transcription regulators (Supplementary Figure S3). Altogether, these observations indicate that dH1 has a global contribution to the regulation of gene expression, affecting expression of both active and inactive genes.

dH1 depletion preferentially affects heterochromatic genes

Approximately 92% of DE-genes that change expression by $|FC| > 2.5$ are up-regulated (Figure 1A), suggesting that dH1 has an important contribution to gene silencing. Consistent with this hypothesis, several genes located in peri-centromeric heterochromatin are strongly up-regulated ($|FC| > 2.5$; Table 1 and Supplementary Table S1). As a matter of fact, dH1 depletion preferentially affects expression of heterochromatic genes. Approximately 45% of all heterochromatic genes/sequences analysed in the Affymetrix array are detected differentially expressed by $|FC| > 1.5$, which is in contrast with the reduced percentage of euchromatic genes that are affected to the same extent (Figure 2A, left). A similar situation is observed at

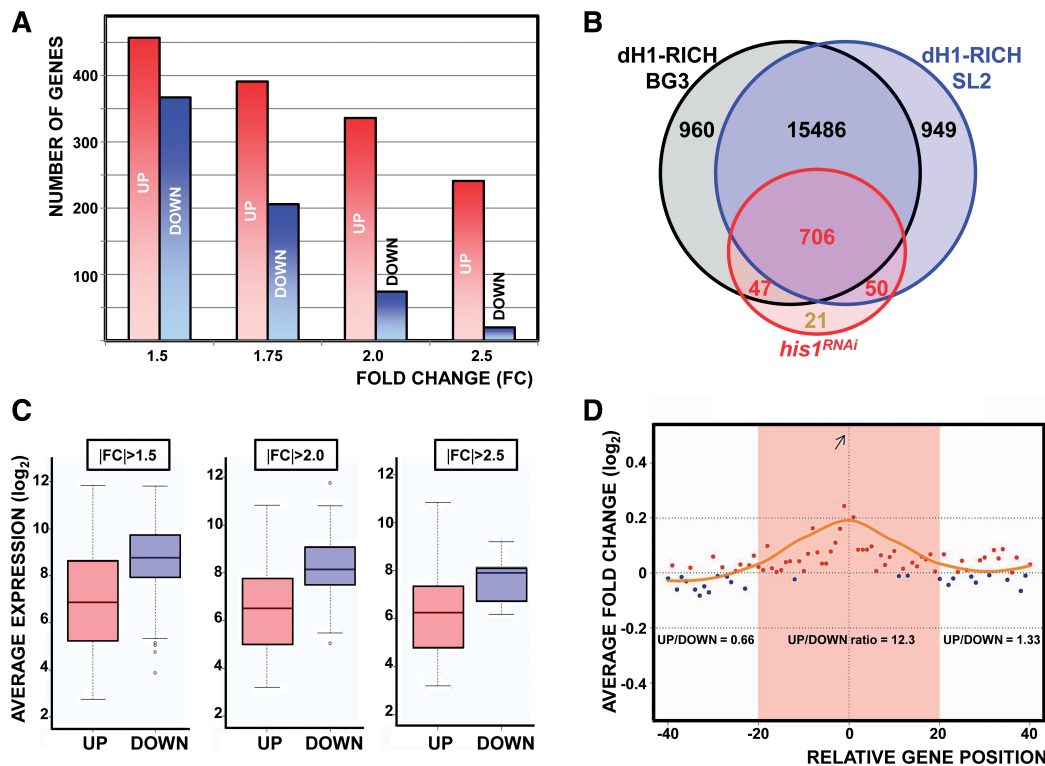


Figure 1. dH1 depletion has a dual effect on gene expression. (A) The number of genes differentially expressed in mutant *his1^{RNAi}; Act5C-GAL4* flies is presented as a function of increasing fold-change (FC) for both up- (red) and down-regulated genes (blue). (B) The overlapping between genes differentially expressed ($|FC| > 1.5$) in mutant *his1^{RNAi}; Act5C-GAL4* flies (red), and dH1-rich regions in S2 (blue) and/or BG3 cells (black) is presented. (C) The average expression in control *GFP^{RNAi}; Act5C-GAL4* flies of genes differentially up- (red) and down-regulated (blue) in mutant *his1^{RNAi}; Act5C-GAL4* flies is presented for the indicated FCs. (D) The average fold change expression in mutant *his1^{RNAi}; Act5C-GAL4* flies is presented for the ±40 genes immediately flanking genes highly differentially expressed ($FC > 2.5$). Up- (red) and down-regulated (blue) genes are indicated. The ratios of the number of up-regulated versus down-regulated genes in the indicated regions are presented.

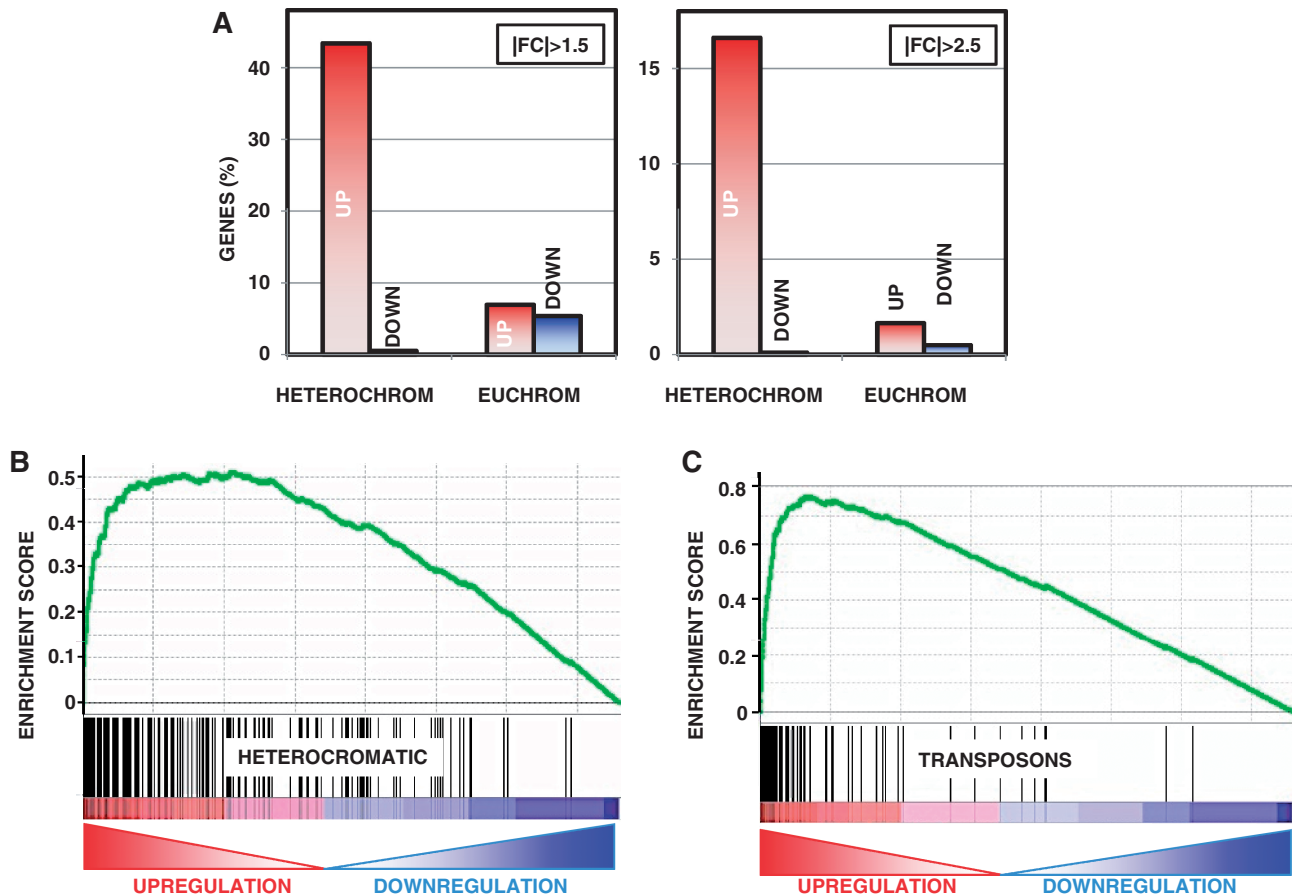


Figure 2. dH1 is required to maintain silencing of heterochromatin genes and transposons. (A) The percentages of heterochromatin and euchromatin genes analyzed in the array that are found differentially expressed in mutant *his1^{RNAi}; Act5C-GAL4* flies are presented for the indicated FCs. Up- (red) and down-regulated genes (blue) are indicated. (B) Gene Set Enrichment Analysis (GSEA) for heterochromatin genes. The distribution of heterochromatin genes (black lines) is presented as a function of the change in expression in mutant *his1^{RNAi}; Act5C-GAL4* knockdown flies, from highly up-regulated (red) to highly down-regulated (blue). Enrichment score is calculated as described under ‘Materials and Methods’ section. (C) As in B but for transposons.

$|FC| > 2.5$ (Figure 2A, right). Note that, while euchromatin genes are detected up- and down-regulated, heterochromatin ones are mainly up-regulated. GSEA confirms these results. In this type of analysis, all genes in the array are ranked according to their change in expression, from the most up-regulated to the most down-regulated. Then, an enrichment-score is calculated to measure the enrichment on heterochromatin genes as a function of the change in expression (see ‘Materials and Methods’ section for details) (40,41). As shown in Figure 2B, heterochromatin genes are significantly enriched amongst up-regulated genes. Altogether, these results indicate that dH1 depletion preferentially affects heterochromatin genes, which is consistent with previous reports showing an essential contribution of dH1 to heterochromatin organization and function in *D. melanogaster* (26).

dH1 is required to maintain silencing of transposons

Among up-regulated DE-genes, we also identified several TE, which include representative examples of all main TE classes of *Drosophila* (Supplementary Table S1). For instance, 10 retrotransposons (7 LTR and 3 LINE-like

elements) are detected up-regulated by $|FC| > 2.5$ (Table 2), and qRT-PCR analyses confirmed these results (Supplementary Figure S4). Furthermore, GSEA shows that TEs are strongly enriched amongst up-regulated genes (Figure 2C). Altogether, these observations indicate that dH1 regulates TEs silencing.

TEs are distributed all across the genome, comprising 4% of euchromatin and ~20% of heterochromatin (45–47). dH1 likely mediates silencing of heterochromatin TEs since, as discussed above, it has a general contribution to silencing of genes located in heterochromatin. However, increased TEs expression detected in the absence of dH1 must also reflect a major contribution to silencing of euchromatin TEs, as ~90% of all functional full-length TE copies are inserted in euchromatin. As a matter of fact, only ~2% of heterochromatin TEs are full-length, compared to 21% in euchromatin (46,47). Consistent with this hypothesis, dH1 is specifically enriched at euchromatin TEs (43). Moreover, dH1 depletion strongly up-regulates expression of R2 (Table 2 and Supplementary Figure S4), a LINE-like retrotransposon that integrates sequence-specifically in the rDNA locus (28–30).

Table 1. List of heterochromatic genes differentially up-regulated by FC > 2.5 in *his1^{RNAi}*

Gene	FC	Localization
CG40467	10.86	3LHet
CG40270	9.94	2RHet
CG40211	9.34	2RHet
CG40155	6.79	3RHet
CG40116	5.58	2RHet
CG41057	5.28	3RHet
Dbp80	4.77	3LHet
l(2)41Ab	4.29	2RHet
Sep1	4.21	2RHet
CG41056	4.15	3RHet
CG17374	3.67	3LHet
CG40062	3.57	2RHet
CG40120	3.48	3LHet
CG40383	3.44	3RHet
CG40216	3.21	2RHet
CG40211	3.15	2RHet
CG2893	3.08	XHet
CG17478	3.08	Het ^a
CG40153	2.98	3RHet
CG40396	2.94	Het ^a
CG40001	2.81	3LHet
CG40130	2.67	Het ^a
CG17702	2.64	2RHet
CG40182	2.58	3RHet

^aNot mapped.**Table 2.** List of transposons differentially up-regulated by FC > 2.5 in *his1^{RNAi}*

Transposon	FC	Class
GYPSY6	6.95	LTR
FROGGER	6.57	LTR
G3	5.72	LINE
ACCORD2	5.44	LTR
R2	4.89	LINE
1731	4.82	LTR
GYPSY5	3.68	LTR
IVK	3.67	LINE
GATE	3.40	LTR
DIVER2	2.95	LTR

Up-regulation of R2 is particularly interesting, as ~11% of rDNA units contain R2 inserted at a specific site of the 28S gene. A second closely related transposon, R1, also integrates sequence-specifically at a different site in ~44% of the 28S rDNA units (30,48). In addition, ~5% of 28S rDNA units contain both R1 and R2. As shown above, R2 is strongly up-regulated upon dH1 depletion (Table 2 and Supplementary Figure S4), and, although probes to detect R1 expression were not present in the Affymetrix array, qRT-PCR experiments showed that R1 is also strongly up-regulated in the absence of dH1 (Figure 3A). rDNA units containing inserted R1 and/or R2, which altogether account for 60% of all rDNA units, are expressed about 5- to 10-fold less than uninserted copies (48). Therefore, we wondered whether dH1 depletion only affects expression of the R1/R2 transposons or the whole inserted rDNA units are up-regulated. For this

purpose, we performed qRT-PCR experiments using primers flanking the 5'-insertion sites of R1 and R2. As shown in Figure 3A, dH1 depletion increases expression of 28S rDNA copies containing R1 and/or R2 by ~4-fold, indicating that rRNA synthesis is strongly up-regulated in the absence of dH1. In good agreement with these results, nucleolar morphology is strongly altered in cells lacking dH1 (Figure 3B and C). In these experiments, nucleolar morphology was analysed by immunostaining with antibodies against fibrillarin, a nucleolar component involved in rRNA processing (49). In comparison with control wild-type cells, depleted cells show enlarged nucleolus both in salivary glands (Figure 3B) and wing imaginal discs (Figure 3C). Consistent with these results, western blot analyses show that, in salivary glands, fibrillarin content increases by ~50% in *his1^{RNAi}* flies (Figure 3D).

dH1 depletion induces genomic instability and affects proliferation

Results reported above indicate that dH1 depletion relieves transposon silencing. In particular, transposons inserted at the rDNA locus are strongly up-regulated, resulting in deregulated expression of the locus and synthesis of aberrant rRNA transcripts. Deregulation of the rDNA locus is known to induce hyper-recombination, causing profound genomic rearrangements that, most often, result in the excision of genomic rDNA copies and the production of extra-chromosomal rDNA circles (*ecc^{rDNA}*) (50,51). In fact, *ecc^{rDNA}* are readily detectable in dH1-depleted cells. In these experiments, Hirt extracts were prepared from salivary glands and imaginal discs, and assayed by qPCR for the presence of *ecc^{rDNA}*. As shown in Figure 4A, in comparison with control wild-type larvae, *ecc^{rDNA}* strongly increases in extracts prepared from dH1-depleted larvae, while no *ecc^{rDNA}* is detected from other loci, indicating that dH1 depletion causes genome instability. Note that a similar increase in *ecc^{rDNA}* is detected in *su(var)3-9⁰⁶* mutants, which are known to strongly affect genome stability (51,52). Consistent with these results, dH1 depletion causes DNA damage, as judged by immunostaining with antibodies against γ H2Av, a specific phosphorylation of histone H2Av that occurs at sites of double-stranded breaks (DSB) (53). As shown in Figure 4B, significant γ H2Av is observed in the pouch after dH1 depletion.

It is well established that DNA damage stops cell proliferation and, ultimately, induces apoptosis (53). In fact, as determined by immunostaining with α H3S10P antibodies, which mark cells undergoing mitosis, the frequency of mitotic cells detected in the pouch is strongly reduced upon dH1 depletion (Figure 5A). Moreover, strong α caspase-3 reactivity is observed (Figure 5B), indicating that depleted cells activate apoptosis. Concomitantly, dH1 depletion in the pouch, which gives rise to the wing, results in strong phenotypes in adult flies that show very small malformed wings (Figure 5C). In good agreement with these results, proliferation of dH1-depleted cells is rescued when apoptosis is blocked by over-expressing p35, a baculovirus protein that is a broad-spectrum caspase inhibitor in nematode, *Drosophila*, and mammalian cells (54–57). For this purpose, *nub-GAL4* was used to

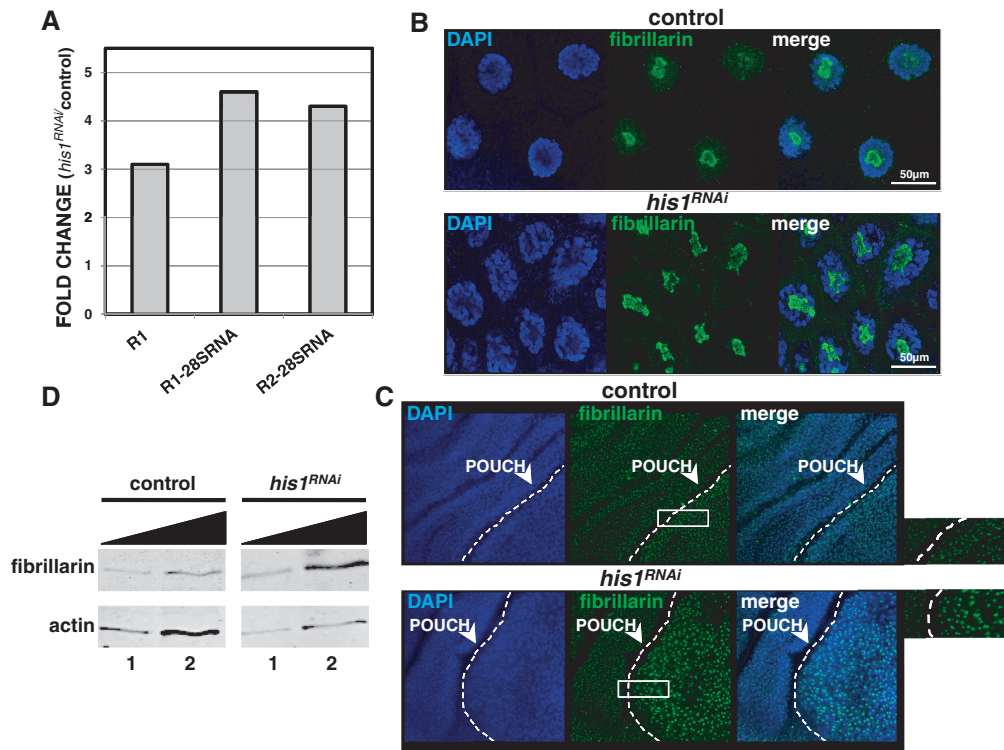


Figure 3. dH1 depletion deregulates expression of the rDNA locus. (A) Quantitative RT-PCR analysis of the levels of expression of R1 retrotransposon, and R1- and R2-inserted 28rRNA copies in mutant *his1^{RNAi}*; *Act5C-GAL4* and control *GFP^{RNAi}*; *Act5C-GAL4* larvae. Total RNA was prepared from wing imaginal discs. Relative expression levels were determined in relation to Rp49 mRNA. Fold change of expression in *his1^{RNAi}* versus control is presented. See Supplementary Table S3 for primers used in these experiments. (B) Nucleolar morphology was determined by immunostaining with α fibrillarins (1:1000; green) in whole salivary glands prepared from mutant *his1^{RNAi}*; *Act5C-GAL4* and control *GFP^{RNAi}*; *Act5C-GAL4* larvae. DNA was stained with DAPI. (C) As in B, but immunostaining was performed in wing imaginal discs prepared from mutant *his1^{RNAi}*; *nub-GAL4*; *UAS_{GAL4}-Der2* and control *GFP^{RNAi}*; *nub-GAL4*; *UAS_{GAL4}-Der2* larvae. The region corresponding to the pouch is indicated. DNA was stained with DAPI. Enlarges images of the indicated regions are shown on the right for easier visualization. (D) Fibrillarins content was analyzed by Western blot using α fibrillarins antibodies (1:1000) in extracts prepared from mutant *his1^{RNAi}*; *Act5C-GAL4* and control *GFP^{RNAi}*; *Act5C-GAL4* salivary glands. Two increasing amounts of extract were analyzed in each case (lanes 1, 2). The signal obtained with α Actin antibodies (1:750) was used as loading control for normalization.

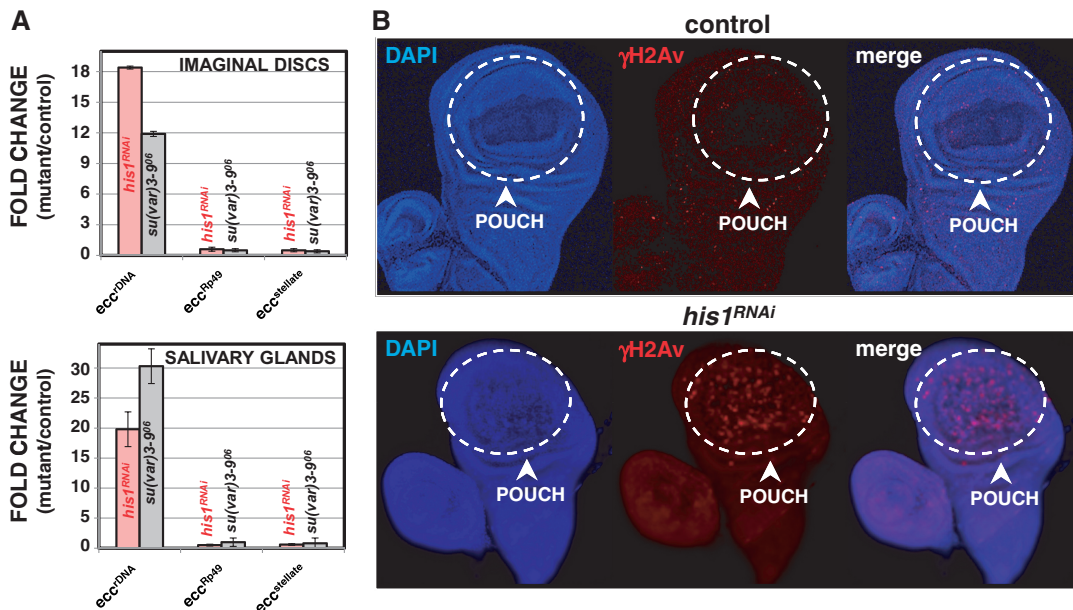


Figure 4. dH1 depletion causes genomic instability. (A) Quantitative PCR analysis of the levels of *ecc^{DNA}* originated from the rDNA, Rp49 or stellate loci in mutant *his1^{RNAi}*; *Act5C-GAL4* and control *GFP^{RNAi}*; *Act5C-GAL4* larvae. Hirt extracts were prepared from imaginal discs (top) and salivary glands (bottom). Fold increase in mutant *his1^{RNAi}* versus control is presented. Similar analyses performed using homozygous *su(var)3-9⁰⁶* larvae are presented as positive controls for comparison. See Supplementary Table S3 for primers used in these experiments. (B) γ H2Av levels were determined by immunostaining using α γ H2Av antibodies (1:1000; red) in wing imaginal discs prepared from mutant *his1^{RNAi}*; *nub-GAL4*; *UAS_{GAL4}-Der2* and control *GFP^{RNAi}*; *nub-GAL4*; *UAS_{GAL4}-Der2* larvae. The region corresponding to the pouch is indicated. DNA was stained with DAPI.

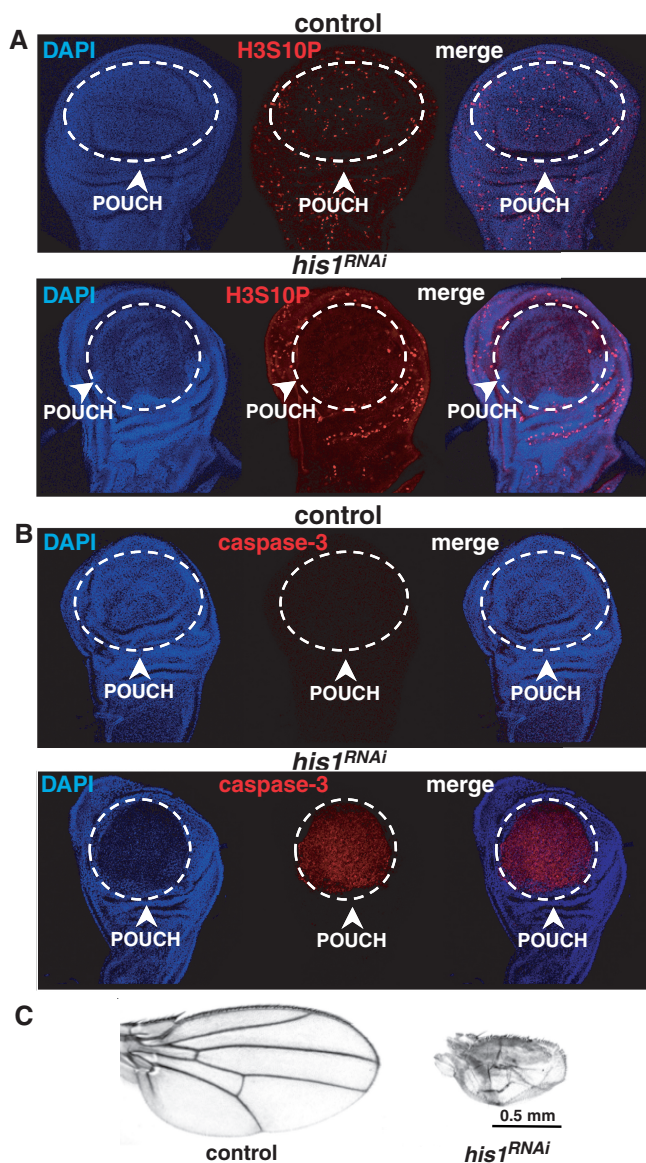


Figure 5. dH1-depleted cells stop proliferation and activate apoptosis. (A) The frequency of mitotic cells was determined by immunostaining using α H3S10P antibodies (1:1000; red) in wing imaginal discs prepared from mutant *his1^{RNAi}*; *nub-GAL4*; *UAS_{GAL4}-Dcr2* and control *GFP^{RNAi}*; *nub-GAL4*; *UAS_{GAL4}-Dcr2* larvae. The region corresponding to the pouch is indicated. DNA was stained with DAPI. (B) Induction of apoptosis was determined by immunostaining using α caspase-3 antibodies (1:1000; red) in wing imaginal discs prepared from mutant *his1^{RNAi}*; *nub-GAL4*; *UAS_{GAL4}-Dcr2* and control *GFP^{RNAi}*; *nub-GAL4*; *UAS_{GAL4}-Dcr2* larvae. The region corresponding to the pouch is indicated. DNA was stained with DAPI. (C) Wings from adult mutant *his1^{RNAi}*; *nub-GAL4*; *UAS_{GAL4}-Dcr2* (right) and control *GFP^{RNAi}*; *nub-GAL4*; *UAS_{GAL4}-Dcr2* flies (left) are presented. In these experiments, *his1^{RNAi}* flies carry a single *UAS_{GAL4}-hsRNA^{His1}* construct inserted in the X-chromosome.

induce dH1 depletion in the pouch and, at the same time, over-expression of p35. Under these conditions, cells in the pouch show significant α H3S10P reactivity (Figure 6B), and wing size is largely recovered (Figure 6C, right). In addition, though reduced with respect to cells capable of undergoing normal apoptosis, depleted cells retained significant γ H2Av (Figure 6A), suggesting that they

proliferate despite accumulating DNA damage. Actually, reflecting their genomic instability, blocking apoptosis results in over-proliferation of dH1-depleted cells, as a high proportion of wing discs show multiple cell layers in the pouch (Supplementary Figure S5) and tumour-like outgrowths are frequently observed in wings of adult flies (Figure 6C, red arrows). It is well established that p35 over-expression by itself does not affect cell proliferation (58). As a matter of fact, control flies over-expressing p35 in the absence of dH1-depletion show normal wings (Figure 6C, left) and no significant γ H2Av is detected in the pouch region (not shown). Similar results were obtained when dH1 depletion was specifically induced at the A/P border, using a *ptc-GAL4* driver (Supplementary Figure S6). Also in this case, dH1 depletion induces γ H2Av (Supplementary Figure S6A), and depleted cells show decreased α H3S10P reactivity (Supplementary Figure S6B) and are positive for caspase-3 (Supplementary Figure S6C). Furthermore, in adult flies, the size of the *ptc*-region is strongly reduced (Supplementary Figure S6D), containing significantly fewer cells than in control flies (Supplementary Figure S6E). Altogether, these results indicate that dH1 depletion induces DNA damage and genomic instability, affecting normal cell proliferation.

Expression of human histone H1 variants partially rescues proliferation of cells lacking dH1

Results discussed above indicate that dH1 depletion causes genomic instability, preventing normal cell proliferation. Next, we asked whether the contribution of dH1 to cell proliferation and the maintenance of genome integrity are conserved functional properties in human hH1s. To address this question, we performed complementation assays, where several hH1 variants were expressed in cells lacking dH1. In these experiments, we used *his1^{RNAi}* flies carrying a UAS-construct expressing human hH1.0, hH1.2 or hH1.4. These flies were crossed to *nub-GAL4* flies to simultaneously induce dH1 depletion and expression of the corresponding hH1 variant in the pouch of wing imaginal discs. Western blot analyses show that, though to somehow different levels, all three hH1 variants are expressed without significantly affecting dH1-depletion (Figure 7A). To assess complementation, we determined the extent to which their expression rescues reduced wing size associated with dH1 depletion. As shown in Figure 7B and C, expression of any of the hH1 variants tested rescues wing defects of *his1^{RNAi}* flies, increasing significantly the average wing length. For instance, very small wings (<0.5 mm) detected in about 30% of *his1^{RNAi}* flies, are not observed in flies expressing hH1 variants (Figure 7D). In addition, depending on the hH1 variant expressed, about 30–75% of flies have long wings (>1.0 mm), which are very infrequent in *his1^{RNAi}* flies (<5%) (Figure 7D). Expression of hH1 variants also rescues lethality associated to dH1 depletion (Supplementary Table S2). Altogether, these results indicate that, though partially, hH1 variants rescue proliferation of cells lacking dH1, suggesting that the contribution of histone H1 to maintenance of genome integrity and cell proliferation are conserved functions in human hH1s.

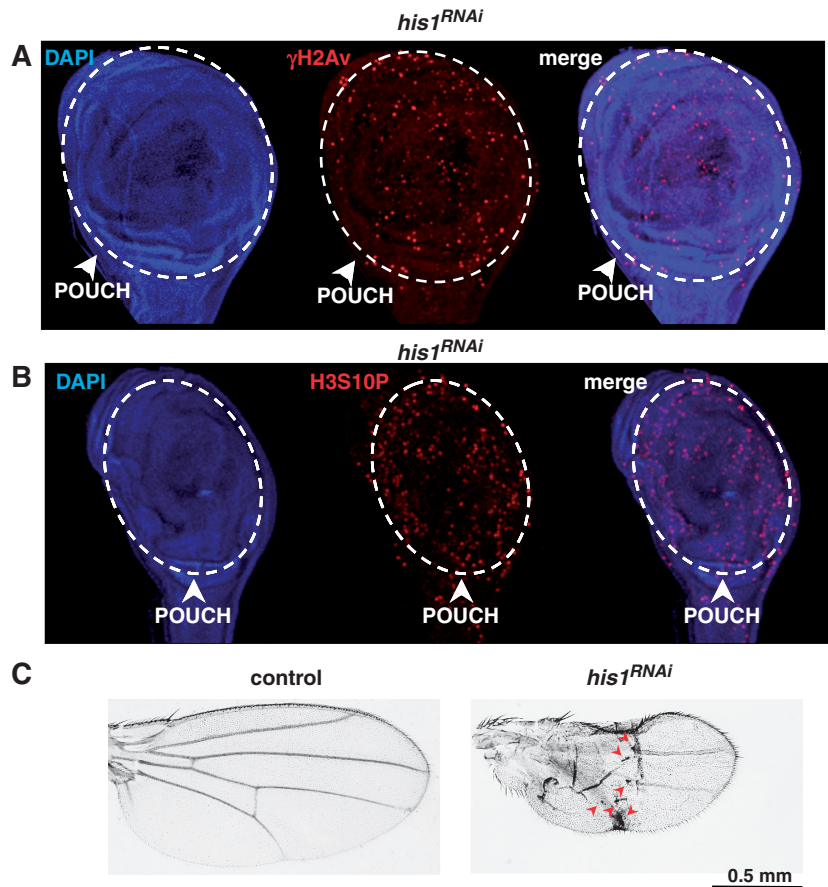


Figure 6. Blocking apoptosis by p35 over-expression rescues proliferation of dH1-depleted cells. (A) γ H2Av levels were determined by immunostaining using $\alpha\gamma$ H2Av antibodies (1:1000; red) in wing imaginal discs prepared from mutant *his1^{RNAi}; nub-GAL4; UAS_{GAL4}-Dcr2; UAS_{GAL4}-p35*. The region corresponding to the pouch is indicated. DNA was stained with DAPI. (B) The frequency of mitotic cells was determined by immunostaining using α H3S10P antibodies (1:1000; red) in wing imaginal discs prepared from mutant *his1^{RNAi}; nub-GAL4; UAS_{GAL4}-Dcr2; UAS_{GAL4}-p35* larvae. The region corresponding to the pouch is indicated. DNA was stained with DAPI. (C) Wings from adult mutant *his1^{RNAi}; nub-GAL4; UAS_{GAL4}-Dcr2; UAS_{GAL4}-p35* (right) and control *GFP^{RNAi}; nub-GAL4; UAS_{GAL4}-Dcr2; UAS_{GAL4}-p35* flies (left) are presented. Red arrows indicate tumour-like outgrowths. In these experiments, *his1^{RNAi}* flies carry a single UAS_{GAL4}-hsRNA^{*His1*} construct inserted in the X-chromosome.

DISCUSSION

Our results show that, despite dH1 is uniformly distributed throughout chromatin (43,44), its depletion affects gene expression only moderately, as <5% of genes change expression by $|FC| > 1.5$. In addition, dH1 depletion has a dual effect on gene expression: up-regulates inactive genes and down-regulates active ones. It could be argued that these relatively mild effects are due to incomplete dH1 depletion. It must be noticed, however, that our expression-profiling experiments were performed under conditions of very strong depletion (90%). Actually, depletion is likely to be even higher over most of the genome since, under similar conditions, others have reported that residual dH1 is unevenly distributed in polytene chromosomes, being concentrated over short genomic regions (26). Furthermore, also in vertebrates, histone H1 depletion affects only a small number of genes, which are both up- and down-regulated (23,59,60), and, in *S. cerevisiae*, deletion of *Hho1* causes only a slight decrease in expression of very few genes (12–14). On the other hand, it is well established that

histone H1 plays a major structural role in chromatin, as it mediates folding of nucleosomes *in vitro* (1–8), and is required for normal nucleosome spacing and chromatin condensation *in vivo* (23,26,59,61). Altogether, these observations strongly suggest that, rather than as a classical transcription factor, histone H1 acts as a structural factor that organises genes in an appropriate configuration for their proper regulation. Consistent with this hypothesis, dH1 affects gene expression in a regional manner. In the absence of dH1, many low-expressed/inactive genes are up-regulated. At this respect, dH1 occupancy appears to be low around transcription start sites (TSS) of active genes (43,44), suggesting that, at promoters, chromatin unfolds to allow access of the transcription machinery. In this context, dH1 depletion could destabilise folding of the nucleofilament at promoters of low-expressed/inactive genes, rendering them more accessible for transcription, and thus accounting for the general up-regulation observed in the absence of dH1. On the other hand, dH1 depletion down-regulates expression of active genes. At this respect, it must be noted that, though

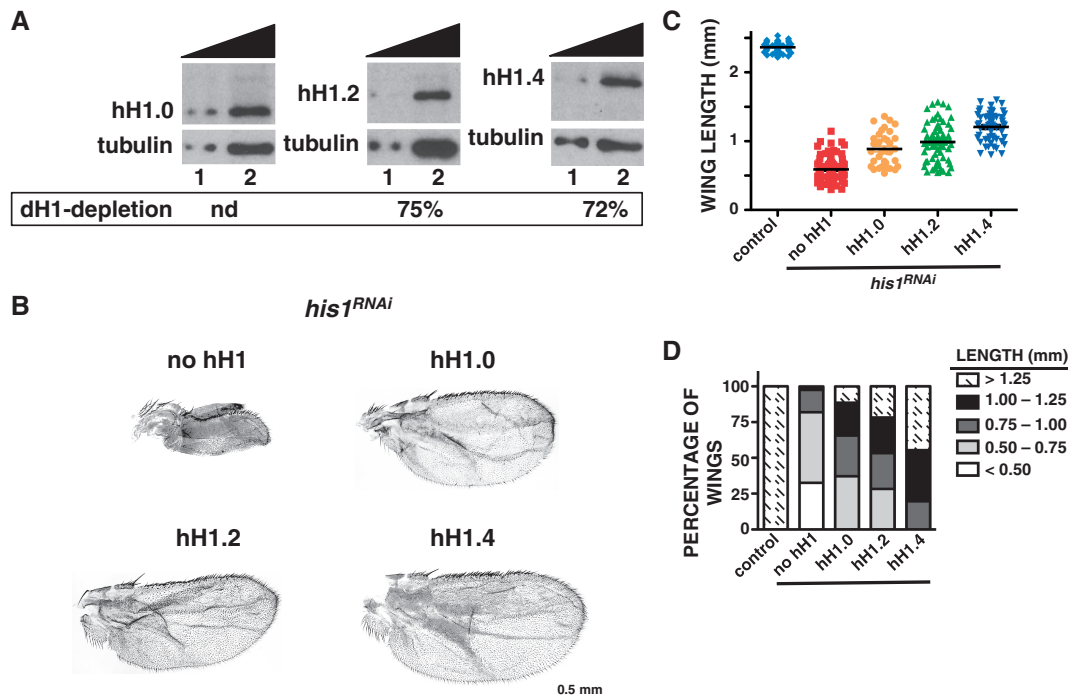


Figure 7. Expression of human hH1 variants rescues proliferation of dH1-depleted cells. **(A)** Levels of expression of HA-tagged hH1.0, hH1.2 and hH1.4 were determined by Western blot using α HA antibodies (1:500) in wing imaginal discs extracts prepared from mutant *his1^{RNAi}; nub-GAL4; UAS_{GAL4}-Dcr2* larvae carrying UAS_{GAL4}-constructs to over-express the indicated hH1 variant. Two increasing amounts of extract were analyzed in each case (lanes 1, 2). The signal obtained with α Tubulin antibodies (1:2000) was used as loading control for normalization. The extent of dH1 depletion (%) determined by Western blot analysis is indicated. **(B)** Wings from adult mutant *his1^{RNAi}; nub-GAL4; UAS_{GAL4}-Dcr2* flies carrying UAS_{GAL4}-constructs to express the indicated hH1 variant or none (no hH1) are presented. **(C)** Average wing length is presented for mutant *his1^{RNAi}; nub-GAL4; UAS_{GAL4}-Dcr2* flies carrying UAS_{GAL4}-constructs to express the indicated hH1 variant or none (no hH1), and for control *GFP^{RNAi}; nub-GAL4; UAS_{GAL4}-Dcr2* flies. **(D)** Percentage of flies showing wings of the indicated lengths is presented for mutant *his1^{RNAi}; nub-GAL4; UAS_{GAL4}-Dcr2* flies carrying UAS_{GAL4}-constructs to express the indicated hH1 variant or not (no hH1), and for control *GFP^{RNAi}; nub-GAL4; UAS_{GAL4}-Dcr2* flies. In these experiments, *his1^{RNAi}* flies carry a single UAS_{GAL4}-hsRNA^{*His1*} construct inserted in the X-chromosome.

lower than at intergenic regions and inactive genes, dH1 content across transcribed regions is significantly higher than at TSS (43,44), suggesting that during transcription elongation chromatin is subjected to folding/unfolding cycles. At present, it is well established that chromatin structure regulates RNA splicing (62). Therefore, it is possible that, at transcribed genes, folding of chromatin facilitates RNA processing. It is also possible that folding of chromatin prevents, and/or destabilises, interactions between nascent transcripts and chromatin that might disturb transcription. Actually, strand displacement by nascent RNA has been shown to result in the formation of R-loops and, most remarkably, mutations that stabilise such structures cause DNA damage and genomic instability, like dH1 depletion does (63–67).

Our results also show that dH1 depletion preferentially affects silencing of genes embedded in peri-centromeric heterochromatin as well as TEs. It is interesting to note that dH1 is enriched at both heterochromatin and TEs (26,43). These observations strongly suggest a specific contribution of dH1 to gene silencing. Consistent with a role in gene silencing, dH1 is a strong suppressor of position-effect variegation and, in addition, its depletion abrogates H3K9me2 at heterochromatin (26). However, the molecular mechanisms of the contribution of dH1 to silencing are not fully understood, as dH1 depletion does

not significantly diminish binding of HP1 to heterochromatin (26), and, on the other hand, transcriptional silencing of TEs in somatic cells appears to involve both HP1-dependent and -independent mechanisms (68–71).

dH1 depletion causes DNA damage and genomic instability that, at least in part, is the consequence of deregulated expression of the rDNA locus due to activation of R1/R2 retrotransposons that are inserted in around 60% of rDNA units (30,48). rDNA replication is tightly regulated to prevent collision with transcription running in the opposite direction. Deregulated transcription of the rDNA locus results in frequent collisions that block replication-fork progression, inducing hyper-recombination, and causing DNA damage and genomic instability (50,51,72,73). It is unlikely that genomic instability of dH1-depleted cells is constrained to the rDNA locus, as dH1 depletion promotes general TEs activation, which induces mutations and can result in genomic instability. In addition, dH1 depletion alters heterochromatin structure (26), which is also known to induce genomic instability (74). Therefore, it is possible that dH1 depletion also induces genomic instability at heterochromatin and TEs. Interestingly, like the rDNA locus, heterochromatin and TEs are regions where DNA replication is more difficult, suggesting that, also at these loci, instability is linked to problems during DNA replication. Actually, in fission yeast, γ H2A accumulates during DNA replication

at rDNA, TEs and heterochromatin (75), and mutations that affect TEs expression cause genomic instability (76). In this context, it is tempting to speculate that genomic instability induced by dH1 depletion is mainly associated with DNA replication. It is possible that, at regions where DNA replication slows down, increased transcription due to dH1 depletion blocks replication-fork progression, causing DNA damage and genomic instability. Interestingly, genomic instability caused by R-loop formation is mainly a consequence of replication-fork collapse (63–66).

Cells lacking dH1 stop proliferating and die through apoptosis. Our results show that, at least in part, these effects are the consequence of DNA damage. We have also shown that expression of three different human hH1 variants rescues proliferation defects associated with dH1 depletion, strongly suggesting that the contributions to proliferation and genome stability are conserved functional properties of histone H1 in metazoans. Actually, depletion of specific human hH1 variants has also been shown to affect proliferation in various human cancer cell lines (23). Interestingly, in these cases, the actual outcome appears to depend on the presence of an intact p53 pathway. For instance, depletion of hH1.2 induces apoptosis in MCF7 cells, which are p53-positives, while it results in G1 arrest in T47D cells, which are p53-negative. Similarly, H1-null chicken DT40 cells, which are also p53-negative, show only minor proliferation defects (61). Altogether, these observations are consistent with a model by which histone H1 depletion induces p53-dependent apoptosis in response to DNA damage. However, we cannot exclude that other factors also contribute to apoptosis induced by dH1 depletion. As a matter of fact, dH1 depletion significantly up-regulates expression of *reaper*, a pro-apoptotic gene (Supplementary Table S1) (77).

SUPPLEMENTARY DATA

Supplementary Data are available at NAR Online: Supplementary Tables 1–3 and Supplementary Figures 1–6.

ACKNOWLEDGEMENTS

We are thankful to Drs J. Kadonaga, M.L. Espinás and A. Jordan for materials and to Drs E. Mejía and A. Jordan for comments on the manuscript. We are also thankful to Mrs E. Fuentes, E. Freire and A. Vera for technical assistance.

FUNDING

MICINN (CSD2006-49 and BFU2009-07111); CSIC (200420E583 and 201120E001); Generalitat de Catalunya (SGR2009-1023); IRB fellowship (to O.V.). This work was carried out within the framework of the 'Centre de Referència en Biotecnologia' of the 'Generalitat de Catalunya'. Funding for open access charge: MICINN.

Conflict of interest statement. None declared.

REFERENCES

- Bassett, A., Cooper, S., Wu, C. and Travers, A. (2009) The folding and unfolding of eukaryotic chromatin. *Curr. Opin. Genet. Dev.*, **19**, 159–165.
- Kasinky, H.E., Lewis, J.D., Dacks, J.B. and Ausio, J. (2001) Origin of H1 linker histones. *FASEB J.*, **15**, 34–42.
- Ramakrishnan, V. (1997) Histone H1 and chromatin higher-order structure. *Crit. Rev. Eukaryot. Gene Expr.*, **7**, 215–230.
- Ramakrishnan, V. (1997) Histone structure and the organization of the nucleosome. *Annu. Rev. Biophys. Biomol. Struct.*, **26**, 83–112.
- Robinson, P.J.J. and Rhodes, D. (2006) Structure of the '30 nm' chromatin fibre: a key role for the linker histone. *Curr. Opin. Struct. Biol.*, **16**, 336–343.
- van Holde, K. and Zlatanova, J. (1996) What determines the folding of the chromatin fiber. *Proc. Natl Acad. Sci. USA*, **93**, 10548–10555.
- van Holde, K.E. (1989) *Chromatin*. Springer, New York.
- Happel, N. and Doenecke, D. (2009) Histone H1 and its isoforms: contribution to chromatin structure and function. *Gene*, **431**, 1–12.
- Laybourn, P.J. and Kadonaga, J.T. (1991) Role of nucleosomal cores and histone H1 in regulation of transcription by RNA polymerase II. *Science*, **254**, 238–245.
- Pennings, S., Meersseman, G. and Bradbury, E.M. (1994) Linker histones H1 and H5 prevent the mobility of positioned nucleosomes. *Proc. Natl Acad. Sci. USA*, **91**, 10275–10279.
- Shimamura, A., Sapp, M., Rodriguez-Campos, A. and Worcel, A. (1989) Histone H1 represses transcription from minichromosomes assembled in vitro. *Mol. Cell. Biol.*, **9**, 5573–5584.
- Downs, J.A., Kosmidou, E., Morgan, A. and Jackson, S.P. (2003) Suppression of homologous recombination by the *Saccharomyces cerevisiae* linker histone. *Mol. Cell*, **11**, 1685–1692.
- Hellauer, K., Sirard, E. and Turcotte, B. (2001) Decreased expression of specific genes in yeast cells lacking histone H1. *J. Biol. Chem.*, **276**, 13587–13592.
- Patterson, H.G., Landel, C.C., Landsman, D., Peterson, C.L. and Simpson, R.T. (1998) The biochemical and phenotypic characterization of Hho1p, the putative linker histone H1 of *Saccharomyces cerevisiae*. *J. Biol. Chem.*, **273**, 7268–7276.
- Ramón, A., Muro-Pastor, M.I., Scazzocchio, C. and Gonzalez, R. (2000) Deletion of the unique gene encoding a typical histone H1 has no apparent phenotype in *Aspergillus nidulans*. *Mol. Microbiol.*, **35**, 223–233.
- Shen, X., Yu, L., Weir, J.W. and Gorovsky, M.A. (1995) Linker histones are not essential and affect chromatin condensation in vivo. *Cell*, **82**, 47–56.
- Mariño-Ramírez, L., Hsu, B., Baxenavis, A.D. and Landsman, D. (2006) The histone database: a comprehensive resource for histones and histone fold-containing proteins. *Proteins*, **62**, 838–842.
- Fan, Y., Sirotkin, A., Russell, R.G. and Skoultchi, A.I. (2001) Individual somatic H1 subtypes are dispensable for mouse development even in mice lacking the H1(0) replacement subtype. *Mol. Cell. Biol.*, **21**, 7933–7943.
- Sirotkin, A.M., Edelmann, W., Cheng, G., Klein-Szanto, A., Kucherlapati, R. and Skoultchi, A.I. (1995) Mice develop normally without the H1(0) linker histone. *Proc. Natl Acad. Sci. USA*, **92**, 6434–6438.
- Takami, Y. and Nakayama, T. (1997) One allele of the major histone gene cluster is enough for cell proliferation of the DT40 chicken B cell line. *Biochem. Biophys. Acta*, **1354**, 105–115.
- Takami, Y. and Nakayama, T. (1997) A single copy of linker H1 genes is enough for proliferation of the DT40 chicken B cell line and linker H1 variants participate in regulation of gene expression. *Genes Cell*, **2**, 711–723.
- Fan, Y., Nikitina, T., Morin-Kensicki, E.M., Zhao, J., Magnuson, T.R., Woodcock, C.L. and Skoultchi, A.I. (2003) H1 linker histones are essential for mouse development and affect nucleosome spacing in vivo. *Mol. Cell. Biol.*, **23**, 4559–4572.
- Sancho, M., Diani, E., Beato, M. and Jordan, A. (2008) Depletion of human histone H1 variants uncovers specific roles in gene expression and cell growth. *PLoS Genet.*, **4**, e1000227.

24. Lifton, R.P., Goldberg, M.L., Karp, R.W. and Hogness, D.S. (1978) The organization of the histone genes in *Drosophila melanogaster*: functional and evolutionary implications. *Cold Spring Harb. Symp. Quant. Biol.*, **42**, 1047–1051.
25. Nagel, S. and Grossbach, U. (2000) Histone H1 genes and histone gene clusters in the genus *Drosophila*. *J. Mol. Evol.*, **51**, 286–298.
26. Lu, X., Wontakal, S.N., Emelyanov, A.V., Morcillo, P., Konev, A.Y., Fyodorov, D.V. and Skoultchi, A.I. (2009) Linker histone H1 is essential for *Drosophila* development, the establishment of pericentric heterochromatin, and a normal polytene chromosome structure. *Genes Dev.*, **23**, 452–465.
27. Siriaco, G., Deuring, R., Chioda, M., Becker, P.B. and Tamkun, J.W. (2009) *Drosophila* ISWI regulates the association of histone H1 with interphase chromosomes *in vivo*. *Genetics*, **182**, 661–669.
28. Jakubczak, J.L., Burke, W.D. and Eickbush, T.H. (1991) Retrotransposable elements R1 and R2 interrupt the rRNA genes of most insects. *Proc. Natl Acad. Sci. USA*, **88**, 3295–3299.
29. Jakubczak, J.L., Xiong, Y. and Eickbush, T.H. (1990) Type I (R1) and type II (R2) ribosomal DNA insertions of *Drosophila melanogaster* are retrotransposable elements closely related to those of *Bombyx mori*. *J. Mol. Biol.*, **212**, 37–52.
30. Jakubczak, J.L., Zenni, M.K., Woodruff, R.C. and Eickbush, T.H. (1992) Turnover of R1 (type I) and R2 (type II) retrotransposable elements in the ribosomal DNA of *Drosophila melanogaster*. *Genetics*, **131**, 129–142.
31. Bischof, J., Maeda, R.K., Hediger, M., Karch, F. and Basler, K. (2007) An optimized transgenesis system for *Drosophila* using germ-line-specific phiC31 integrases. *Proc. Natl Acad. Sci. USA*, **104**, 3312–3317.
32. Schotta, G., Ebert, A., Krauss, V., Fischer, A., Hoffmann, J., Rea, S., Jenuwein, T., Dorn, R. and Reuter, G. (2002) Central role of *Drosophila* SU(VAR)3-9 in histone H3-K9 methylation and heterochromatic gene silencing. *EMBO J.*, **21**, 1121–1131.
33. Andres, A.J. and Thummel, C.S. (1994) Methods for quantitative analysis of transcription in larvae and prepupae. *Methods Cell Biol.*, **44**, 565–573.
34. Gentleman, R.C., Carey, V.J., Bates, D.M., Bolstad, B., Dettling, M., Dudoit, S., Ellis, B., Gautier, L., Ge, Y., Gentry, J. *et al.* (2004) Bioconductor: open software development for computational biology and bioinformatics. *Genome Biol.*, **5**, R80.
35. Carvalho, B.S. and Irizarry, R.A. (2010) A framework for oligonucleotide microarray preprocessing. *Bioinformatics*, **26**, 2363–2367.
36. Smyth, G.K. (2005) Limma: linear models for microarray data. In: Gentleman, R., Carey, V., Dudoit, S., Irizarry, R. and Huber, W. (eds), *Bioinformatics and Computational Biology Solutions using R and Bioconductor*. Springer, New York, pp. 397–420.
37. Rossell, D., Guerra, R. and Scott, C. (2008) Semi-parametric differential expression analysis via partial mixture estimation. *Stat. Appl. Genet. Mol.*, **7**, 1–15.
38. Durinck, S., Moreau, Y., Kasprzyk, A., Davis, S., De Moor, B., Brazma, A. and Huber, W. (2005) BioMart and Bioconductor: a powerful link between biological databases and microarray data analysis. *Bioinformatics*, **21**, 3439–3440.
39. Zhu, L., Gazin, C., Lawson, N., Lin, S., Lapointe, D. and Green, M. (2010) ChIPpeakAnno: a Bioconductor package to annotate ChIP-seq and ChIP-chip data. *BMC Bioinformatics*, **11**, 237.
40. Mootha, V.K., Lindgren, C.M., Eriksson, K.F., Subramanian, A., Sihag, S., Lehar, J., Puigserver, P., Carlsson, E., Ridderstråle, M., Laurila, E. *et al.* (2003) PGC-1alpha-responsive genes involved in oxidative phosphorylation are coordinately downregulated in human diabetes. *Nat. Genet.*, **34**, 267–273.
41. Subramanian, A., Tamayo, P., Mootha, V.K., Mukherjee, S., Ebert, B.L., Gillette, M.A., Paulovich, A., Pomeroy, S.L., Golub, T.R., Lander, E.S. *et al.* (2005) Gene set enrichment analysis: a knowledge-based approach for interpreting genome-wide expression profiles. *Proc. Natl Acad. Sci. USA*, **102**, 15545–15550.
42. Font-Burgada, J., Rossell, D., Auer, H. and Azorín, F. (2008) *Drosophila* HP1c isoform interacts with the zinc-finger proteins WOC and Relative-of-WOC to regulate gene expression. *Genes Dev.*, **22**, 3007–3023.
43. Braunschweig, U., Hogan, G.J., Pagie, L. and van Steensel, B. (2009) Histone H1 binding is inhibited by histone variant H3.3. *EMBO J.*, **28**, 3635–3645.
44. Kharchenko, P.V., Alekseyenko, A.A., Schwartz, Y.B., Minoda, A., Riddle, N.C., Ernst, J., Sabo, P.J., Larschan, E., Gorchakov, A.A., Gu, T. *et al.* (2010) Comprehensive analysis of the chromatin landscape in *Drosophila melanogaster*. *Nature*, **471**, 480–485.
45. Bartolomé, C., Maside, X. and Charlesworth, B. (2002) On the abundance and distribution of transposable elements in the genome of *Drosophila melanogaster*. *Mol. Biol. Evol.*, **19**, 926–937.
46. Kaminker, J.S., Bergman, C.M., Kronmiller, B., Carlson, J., Svirskas, R., Patel, S., Frise, E., Wheeler, D.A., Lewis, S.E., Rubin, G.M. *et al.* (2002) The transposable elements of the *Drosophila melanogaster* euchromatin: a genomics perspective. *Genome Biol.*, **3**, research0084.0081-0084.0020.
47. Smith, C.D., Shu, S., Mungall, C.J. and Karpen, G.H. (2007) The release 5.1 annotation of *Drosophila melanogaster* heterochromatin. *Science*, **316**, 1586–1591.
48. Ye, J. and Eickbush, T.H. (2006) Chromatin structure and transcription of the R1- and R2-inserted rRNA genes of *Drosophila melanogaster*. *Mol. Cell Biol.*, **26**, 8781–8790.
49. Tollervey, D., Lehtonen, H., Jansen, R., Kern, H. and Hurt, E.C. (1993) Temperature-sensitive mutations demonstrate roles for yeast fibrillar in pre-rRNA processing, pre-rRNA methylation, and ribosome assembly. *Cell*, **72**, 443–457.
50. Pasero, P., Bensimon, A. and Schwob, E. (2002) Single-molecule analysis reveals clustering and epigenetic regulation of replication origins at the yeast rDNA locus. *Genes Dev.*, **16**, 2479–2484.
51. Peng, J.C. and Karpen, G.H. (2007) H3K9 methylation and RNA interference regulate nucleolar organization and repeated DNA stability. *Nat. Cell Biol.*, **9**, 25–35.
52. Peng, J.C. and Karpen, G.H. (2009) Heterochromatic genome stability requires regulators of histone H3 K9 methylation. *PLoS Genet.*, **5**, e1000435.
53. Lukas, J., Lukas, C. and Bartek, J. (2011) More than just a focus: the chromatin response to DNA damage and its role in genome integrity maintenance. *Nat. Cell Biol.*, **13**, 1161–1169.
54. Clem, R.J., Fechtner, M. and Miller, L.K. (1991) Prevention of apoptosis by a baculovirus gene during infection of insect cells. *Science*, **254**, 1388–1390.
55. Davidson, F.F. and Steller, H. (1998) Blocking apoptosis prevents blindness in *Drosophila* retinal degeneration mutants. *Nature*, **391**, 587–591.
56. Sugimoto, A., Friesen, P.D. and Rothman, J.H. (1994) Baculovirus p35 prevents developmentally programmed cell-death and rescues a ced-9 mutant in the nematode *Caenorhabditis elegans*. *EMBO J.*, **13**, 2023–2028.
57. Viswanath, V., Wu, Z., Fonck, C., Wei, Q., Boonplueang, R. and Andersen, J.K. (2000) Transgenic mice neuronally expressing baculoviral p35 are resistant to diverse types of induced apoptosis, including seizure-associated neurodegeneration. *Proc. Natl Acad. Sci. USA*, **97**, 2270–2275.
58. Martin, F.A., Pérez-Garijo, A. and Morata, G. (2009) Apoptosis in *Drosophila*: compensatory proliferation and undead cells. *Int. J. Dev. Biol.*, **53**, 1341–1347.
59. Fan, Y., Nikitina, T., Zhao, J., Fleury, T.J., Bhattacharyya, R., Bouhassira, E.E., Stein, A., Woodcock, C.L. and Skoultchi, A.I. (2005) Histone H1 depletion in mammals alters global chromatin structure but causes specific changes in gene regulation. *Cell*, **123**, 1199–1212.
60. Takami, Y., Nishi, R. and Nakayama, T. (2000) Histone H1 variants play individual roles in transcription regulation in the DT40 chicken B cell line. *Biochem. Biophys. Res. Commun.*, **268**, 501–508.
61. Washimoto, H., Takami, Y., Sonoda, E., Iwasaki, T., Iwano, H., Tachibana, M., Takeda, S., Nakayama, T., Kimura, H. and Shinkai, Y. (2010) Histone H1 null vertebrate cells exhibit altered nucleosome architecture. *Nucleic Acids Res.*, **38**, 3533–3545.
62. Luco, R.F. and Misteli, T. (2011) More than a splicing code: integrating the role of RNA, chromatin and non-coding RNA in alternative splicing regulation. *Curr. Opin. Genet. Dev.*, **21**, 366–372.

63. Aguilera, A. and Gómez-González, B. (2008) Genome instability: a mechanistic view of its causes and consequences. *Nat. Rev. Genet.*, **9**, 204–217.
64. Gan, W., Guan, Z., Liu, J., Gui, T., Shen, K., Manley, J.L. and Li, X. (2011) R-loop-mediated genomic instability is caused by impairment of replication fork progression. *Genes Dev.*, **25**, 2041–2056.
65. Gómez-González, B., García-Rubio, M., Bermejo, R., Gaillard, H., Shirahige, K., Marín, A., Foiani, M. and Aguilera, A. (2011) Genome-wide function of THO/TREX in active genes prevents R-loop-dependent replication obstacles. *EMBO J.*, **30**, 3106–3119.
66. Huertas, P. and Aguilera, A. (2003) Cotranscriptionally formed DNA:RNA hybrids mediate transcription elongation impairment and transcription-associated recombination. *Mol. Cell*, **12**, 711–721.
67. Luna, R., Gaillard, H., González-Aguilera, C. and Aguilera, A. (2008) Biogenesis of mRNPs: integrating different processes in the eukaryotic nucleus. *Chromosoma*, **117**, 319–331.
68. Fanti, L., Berloco, M., Piacentini, L. and Pimpinelli, S. (2003) Chromosomal distribution of heterochromatin protein 1 (HP1) in *Drosophila*: a cytological map of euchromatic HP1 binding sites. *Genetica*, **117**, 135–147.
69. Fanti, L., Dorer, D.R., Berloco, M., Henikoff, S. and Pimpinelli, S. (1998) Heterochromatin protein 1 binds transgene arrays. *Chromosoma*, **107**, 286–292.
70. Minervini, C.F., Marsano, R.M., Casieri, P., Fanti, L., Caizzi, R., Pimpinelli, S., Rocchi, M. and Viggiano, L. (2007) Heterochromatin protein 1 interacts with 5'UTR of transposable element ZAM in a sequence-specific fashion. *Gene*, **393**, 1–10.
71. Phalke, S., Nickel, O., Walluscheck, D., Hortig, F., Onorati, M.C. and Reuter, G. (2009) Retrotransposon silencing and telomere integrity in somatic cells of *Drosophila* depends on the cytosine-5 methyltransferase DNMT2. *Nat. Genet.*, **41**, 696–702.
72. Kobayashi, T. and Ganley, A.R. (2005) Recombination regulation by transcription-induced cohesin dissociation in rDNA repeats. *Science*, **309**, 1581–1584.
73. Mayan, M. and Aragon, L. (2010) Cis-interactions between non-coding ribosomal spacers dependent on RNAP-II separate RNAP-I and RNAP-III transcription domains. *Cell Cycle*, **9**, 4328–4337.
74. Peng, J.C. and Karpen, G.H. (2008) Epigenetic regulation of heterochromatic DNA stability. *Curr. Opin. Genet. Dev.*, **18**, 204–211.
75. Rozenzhak, S., Mejia-Ramírez, E., Williams, J.S., Schaffer, L., Hammond, J.A., Head, S.R. and Russell, P. (2010) Rad3 decorates critical chromosomal domains with gammaH2A to protect genome integrity during S-Phase in fission yeast. *PLoS Genet.*, **6**, e1001032.
76. Zaratiegui, M., Vaughn, M.W., Irvine, D.V., Goto, D., Watt, S., Bähler, J., Arcangioli, B. and Martienssen, R.A. (2011) CENP-B preserves genome integrity at replication forks paused by retrotransposon LTR. *Nature*, **469**, 112–115.
77. Hay, B.A. and Guo, M. (2006) Caspase-dependent cell death in *Drosophila*. *Ann. Rev. Cell Dev. Biol.*, **22**, 623–650.